

Effect of strain-induced electronic topological transitions on the superconducting properties of $\text{La}_{2-x}\text{Sr}_x\text{CuO}_4$ thin films

G. G. N. Angilella¹, G. Balestrino^{2,5}, P. Cermelli³, P. Podio-Guidugli⁴, and A. A. Varlamov⁵

¹ Dipartimento di Fisica e Astronomia, Università di Catania, and Istituto Nazionale per la Fisica della Materia, UdR di Catania, Corso Italia, 57, I-95129 Catania, Italy

² Dipartimento di Scienze e Tecnologie Fisiche ed Energetiche, Università di Roma “Tor Vergata”, Via di Tor Vergata, 110, I-00133 Roma, Italy

³ Dipartimento di Matematica, Università di Torino, Via Carlo Alberto, 10, I-10123 Torino, Italy

⁴ Dipartimento di Ingegneria Civile, Università di Roma “Tor Vergata”, Via di Tor Vergata, 110, I-00133 Roma, Italy

⁵ Istituto Nazionale per la Fisica della Materia, UdR di Tor Vergata, Via di Tor Vergata, 110, I-00133 Roma, Italy

October 27, 2018

Abstract. We propose a Ginzburg-Landau phenomenological model for the dependence of the critical temperature on microscopic strain in tetragonal high- T_c cuprates. Such a model is in agreement with the experimental results for LSCO under epitaxial strain, as well as with the hydrostatic pressure dependence of T_c in most cuprates. In particular, a nonmonotonic dependence of T_c on hydrostatic pressure, as well as on in-plane or apical microstrain, is derived. From a microscopic point of view, such results can be understood as due to the proximity to an electronic topological transition (ETT). In the case of LSCO, we argue that such an ETT can be driven by a strain-induced modification of the band structure, at constant hole content, at variance with a doping-induced ETT, as is usually assumed.

PACS. 74.62.Fj Transition temperature variations; pressure effects – 74.20.De Phenomenological theories (two-fluid, Ginzburg-Landau, etc.) – 74.72.Dn La-based cuprates

1 Introduction

The application of high pressure to high- T_c cuprate superconductors (HTS) is known to modify remarkably the superconducting properties of these materials [1]. In particular, it was shown by Gao *et al.* [2] that quasi-hydrostatic pressure can increase the critical temperature of $\text{HgBa}_2\text{Ca}_2\text{Cu}_3\text{O}_{8+\delta}$ up to about 164 K. Such a record has been very recently challenged, by achieving $T_c = 117$ K in C_{60} single crystals, where an expansion of the crystalline lattice was realized via the intercalation of CHCl_3 and CHBr_3 (chemical pressure) [3]. Even more promising is the possibility of increasing T_c in HTS thin films via the anisotropic strain induced by epitaxial growth on mismatching substrates. The effect of tensile and compressive epitaxial strains on the transport properties has been investigated. This research has been mostly focused on the $\text{La}_{2-x}\text{Sr}_x\text{CuO}_4$ (LSCO) compound because in this system the hole concentration is well controlled over an exceptionally wide range, and mostly determined by the Sr content (together with small oxygen non-stoichiometry). Using SrLaAlO_4 (SLAO) substrates (with in-plane lattice spacing $a = 3.755$ Å), epitaxial LSCO films ($a = 3.777$ Å) have been grown which were in-plane compressively strained [4]. Critical temperatures as high as 49 K have been obtained in slightly underdoped $\text{La}_{2-x}\text{Sr}_x\text{CuO}_4$

with $x = 0.11$ [5], and $T_c = 44$ K in the same compound, at optimal doping ($x = 0.15$) [6]. Recently, it has been shown that a compressive epitaxial strain can induce an insulator-superconductor transition in undoped or slightly doped La_2CuO_4 films [7]. Such an epitaxial-strain-induced transition is a further dramatic demonstration of the significance of strain in HTS materials.

Different mechanisms have been proposed to explain the dependence of T_c on lattice strain [8,9,10]. A simple explanation is based on the possible dependence on strain of the oxygen excess in the LSCO structure. However, it has been shown in Ref. [11] that this cannot be the only explanation. There is now a general agreement that a key to understanding the relationship between epitaxial strain and superconducting properties is the microstrain associated to certain parameters describing the fine structure of the LSCO cell. Locquet *et al.* [5] have recently suggested that the most relevant microparameter is the distance between the Cu ions in the CuO_2 planes and the apical oxygen.

A phenomenological model accounting for the role of the apical distance has been developed in Ref. [12]; this model, which accounts also for other microparameters, is based on a Ginzburg-Landau approach. Needless to say, no phenomenological model could by itself clarify the physical

mechanism connecting microstrains and superconducting properties. Yet, in our opinion, a result of Ref. [12] offers a clue for a possible explanation: we refer to the prediction, compatible with the available experimental data for LSCO, that the critical temperature is a nonlinear function of the epitaxial strain ε_{epi} in the experimentally accessible range $-0.006 \leq \varepsilon_{\text{epi}} \leq 0.006$. This prediction is directly reminiscent, for reasons that we now detail, of a general prediction of the theory of electronic topological transitions (ETT) [13, 14, 15].

The effect of an ETT on the superconducting properties of quasi-2D systems, such as HTS materials, has attracted renewed interest [16, 17]. It is known that optimally-doped HTS materials are in the proximity of an ETT from a hole-like to an electron-like Fermi surface; in the case of LSCO, angle-resolved photoemission spectroscopy (ARPES) has shown that such a transition occurs for $x \simeq 0.2$ (slightly overdoped samples) [18]. Now, an ETT can be driven, in addition to doping, by a number of different external agents, such as impurity concentration, hydrostatic pressure and, as we here surmise, anisotropic strain. In Ref. [19, 20], the dependence of the critical temperature T_c on the parameter z measuring the deviation of the chemical potential from the ETT was studied, and found to be nonmonotonic. In this paper, we propose that the physical mechanism at the origin of the change in the critical temperature in LSCO films under epitaxial strain is an ETT, driven by microstructural deformations. Furthermore, we show that the nonmonotonic behavior, predicted in the ETT scenario, is in agreement with the behavior foreseen by the phenomenological model of Ref. [12].

The outline of the paper is as follows. After a brief review of the Ginzburg-Landau phenomenological model of Ref. [12], relating T_c to the epitaxial strain ε_{epi} (Sec. 2), we introduce a generic microscopic model for a superconducting electron system on a square lattice, close to an ETT (Sec. 3). Our numerical results are presented in Sec. 4, where a nonmonotonic dependence for T_c as a function of hole doping and band structure is recognized, in agreement with the phenomenological model of Sec. 2. Conclusions and directions for future work are the subject of Sec. 5.

2 Phenomenological model

Experimental data show that, in high- T_c materials such as YBCO and LSCO, the critical temperature has a parabolic dependence on applied hydrostatic pressure: as pressure increases, so does T_c until it reaches a maximum, after which it decreases [1]. Different trends have also been recorded (notably, in orthorhombic YBCO) for T_c as a function of uniaxial strain [21, 22]. These have been interpreted as evidence for the importance of the internal strains, especially in non-tetragonal compounds [23]. Moreover, the role of oxygen relaxation processes in establishing hysteresis loops in the pressure-temperature history of YBCO has been emphasized [24]. On the other hand, such subtleties in the pressure dependence of T_c can be neglected in tetragonal LSCO [25], whose hole content is

mainly determined by the amount of doping Sr. Therefore, LSCO in the tetragonal phase is an ideal candidate to study the dependence of T_c on applied pressure, without (much of) the complication arising from pressure-induced charge rearrangements.

Here, we show that a nonmonotonic dependence of T_c on applied pressure is predicted by a modified Ginzburg-Landau model, which takes into account the dependence of T_c on the lengths of the apical and planar Cu-O bonds. This model has been first introduced for application to LSCO films under epitaxial strain [12]. Remarkably, the predicted behavior of these films is similar: for an increasing, *compressive* epitaxial strain, the critical temperature rises to a maximum, then it decreases.

Tetragonal LSCO has a perovskite lattice structure, with the Cu atoms in octahedral coordination with the O atoms. We denote by $(\text{Cu-O})^a$ and $(\text{Cu-O})^b$ the Cu-O distances in the ab plane (*viz.*, the half-diagonals of the Cu-O octahedron in that atomic plane), and by $(\text{Cu-O})^{\text{api}}$ the apical distance (*viz.*, the half-diagonal of the Cu-O octahedron in the direction of the c axis). We also introduce the *microscopic strain measures*

$$p_a := \frac{(\text{Cu-O})^a - (\text{Cu-O})_0^a}{(\text{Cu-O})_0^a}, \quad (1a)$$

$$p_b := \frac{(\text{Cu-O})^b - (\text{Cu-O})_0^b}{(\text{Cu-O})_0^b}, \quad (1b)$$

$$p_{\text{api}} := \frac{(\text{Cu-O})^{\text{api}} - (\text{Cu-O})_0^{\text{api}}}{(\text{Cu-O})_0^{\text{api}}}, \quad (1c)$$

where $(\text{Cu-O})_0^a$, $(\text{Cu-O})_0^b$, and $(\text{Cu-O})_0^{\text{api}}$ are reference values for the corresponding interatomic distances. We let ε denote the *macroscopic strain tensor*, with components ε_{aa} , ε_{bb} , etc.: ε measures the overall strain of the unit cell, whereas the microscopic strains measure relative changes in the interatomic distances within the cell.

For φ the superelectron density, we write the Ginzburg-Landau free energy as

$$G = G_0(T, \varepsilon) + a_0 \alpha(T, p_a, p_b, p_{\text{api}}) \varphi^2 + b_0 \varphi^4, \quad (2)$$

where $a_0, b_0 > 0$ are constants, and the function α accounts for the dependence of the critical temperature on the Cu-O distances. To fix the ideas, we assume a quadratic dependence, in the form

$$\begin{aligned} \alpha(T, p_a, p_b, p_{\text{api}}) = & T - T_c^0 - \lambda_1(p_a + p_b) - \mu_1(p_a^2 + p_b^2) \\ & - \lambda_2 p_{\text{api}} - \mu_2 p_{\text{api}}^2 - \sigma(p_a + p_b)p_{\text{api}}. \end{aligned} \quad (3)$$

As is well known, the vanishing of α determines the critical temperature:

$$\begin{aligned} T_c = & T_c^0 + \lambda_1(p_a + p_b) + \mu_1(p_a^2 + p_b^2) \\ & + \lambda_2 p_{\text{api}} + \mu_2 p_{\text{api}}^2 + \sigma(p_a + p_b)p_{\text{api}}. \end{aligned} \quad (4)$$

We estimate the phenomenological coefficients λ_i , μ_i and σ from the available experimental data for LSCO under strain. Our procedure consists of two steps: (i) we determine how the microstrains $(p_a, p_b, p_{\text{api}})$ depend on the

	$\lambda_i \times 10^{-3}$	$\mu_i \times 10^{-3}$	$\sigma \times 10^{-3}$
$i = 1$	3.962	-579.664	5
$i = 2$	5.028	-42.029	-

Table 1. Calculated coefficients (in K) for the dependence of T_c on the changes of dimensions of the CuO octahedron, Eq. (4).

macroscopic strain ε ; (ii) we express the critical temperature in Eq. (4) as a function of the strain ε and fit the resulting expression to the available data on strain and T_c .

Step (i) has been performed in Ref. [12], on the basis of the experimental findings of Locquet *et al.* [26] for the variation of the interatomic distances in epitaxially strained thin films of LSCO. In the tetragonal phase, it is reasonable to assume that $p_a = \varepsilon_{aa}$, $p_b = \varepsilon_{bb}$, but the experimental data in Ref. [26] show that p_{api} is a highly non-linear function of the principal strains $(\varepsilon_{aa}, \varepsilon_{bb}, \varepsilon_{cc})$. The actual analytical expression for $p_{\text{api}} = \tilde{p}_{\text{api}}(\varepsilon_{aa}, \varepsilon_{bb}, \varepsilon_{cc})$, interpolating the data in Ref. [26], has been determined in Ref. [12].

Step (ii) corresponds to substituting into Eq. (4) the expressions for $(p_a, p_b, p_{\text{api}})$ in terms of $(\varepsilon_{aa}, \varepsilon_{bb}, \varepsilon_{cc})$. The result is an expression of the form

$$\begin{aligned}
 T_c &= \tilde{T}_c(\varepsilon_{aa}, \varepsilon_{bb}, \varepsilon_{cc}) \\
 &= T_c^0 + \lambda_1(\varepsilon_{aa} + \varepsilon_{bb}) + \mu_1(\varepsilon_{aa}^2 + \varepsilon_{bb}^2) \\
 &\quad + \lambda_2 \tilde{p}_{\text{api}}(\varepsilon_{aa}, \varepsilon_{bb}, \varepsilon_{cc}) + \mu_2 \tilde{p}_{\text{api}}^2(\varepsilon_{aa}, \varepsilon_{bb}, \varepsilon_{cc}) \\
 &\quad + \sigma(\varepsilon_{aa} + \varepsilon_{bb}) \tilde{p}_{\text{api}}(\varepsilon_{aa}, \varepsilon_{bb}, \varepsilon_{cc}), \quad (5)
 \end{aligned}$$

which still contains the unknown coefficients λ_i , μ_i , and σ . These parameters may be determined by fitting the expression (5) to the experimental data on the dependence of the critical temperature under strain [12]. Using the data in Ref. [5, 21, 26, 22, 27], we obtain the values listed in Table 1.

Remark 1 At first order in $(p_a, p_b, p_{\text{api}})$, only the linear terms are important, and the expression (4) reduces to

$$T_c \sim T_c^0 + [4(p_a + p_b) + 5p_{\text{api}}] \times 10^3, \quad (6)$$

which shows that the critical temperature increases with the size of the Cu–O octahedron, and is nearly isotropic in the horizontal and vertical microstrains.

Remark 2 More importantly, for p_{api} fixed, the critical temperature reaches a maximum in correspondence of a given horizontal microstrain $p_a = p_b = p_a^{\text{max}}$, and then it starts decreasing (Fig. 1). A completely analogous behavior takes place for p_a and p_b fixed: the critical temperature reaches a maximum at a given apical microstrain $p_{\text{api}} = p_{\text{api}}^{\text{max}}$ (Fig. 2).

Remark 3 Under epitaxial strain, $\varepsilon_{aa} = \varepsilon_{bb} = \varepsilon_{\text{epi}}$, and $\varepsilon_{cc} = -2(c_{13}/c_{33})\varepsilon_{\text{epi}}$ (c_{13} and c_{33} are components of the constant elasticity tensor of the film [12]), so that the critical temperature in (5) is a function of the epitaxial strain

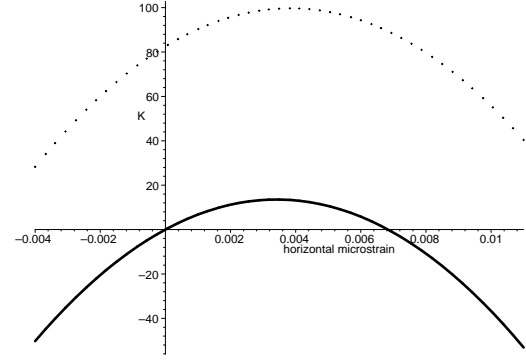


Fig. 1. Theoretical variation of the critical temperature $T_c - T_c^0$ (in K) on the planar microstrain p_a , for two fixed values of the apical microstrain, $p_{\text{api}} = 0$ (solid line), and $p_{\text{api}} = 0.1$ (dotted line), according to Eq. (4).

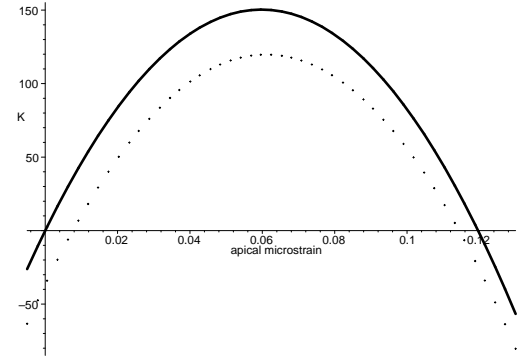


Fig. 2. Theoretical variation of the critical temperature $T_c - T_c^0$ (in K) on the apical microstrain p_{api} , for two fixed values of the planar microstrain, $p_a = 0$ (solid line), and $p_a = 0.01$ (dotted line), according to Eq. (4).

ε_{epi} only. This function is plotted in Fig. 3. Note that T_c is monotonically decreasing in the experimentally accessible range $-0.006 \leq \varepsilon_{\text{epi}} \leq 0.006$, but shows a sharp maximum just below the lower bound of this interval: the predicted values of the maximum T_c are not very far from the experimentally accessible interval, where the quadratic approximation in (4) may still be expected to hold. Thus, the prediction of the phenomenological model seems reasonable.

Remark 4 Under an applied hydrostatic pressure P , we have

$$\varepsilon_{aa} = \varepsilon_{bb} = \frac{(-c_{33} + c_{13})P}{c_{11}c_{33} - 2c_{13}^2 + c_{12}c_{33}}, \quad (7a)$$

$$\varepsilon_{cc} = -\frac{(c_{11} - 2c_{13} + c_{12})P}{c_{11}c_{33} - 2c_{13}^2 + c_{12}c_{33}}, \quad (7b)$$

and the remaining strain components vanish. The critical temperature in (5) becomes a function of the applied

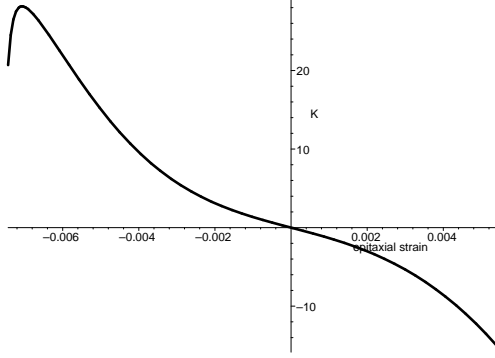


Fig. 3. Theoretical variation of the critical temperature $T_c - T_c^0$ (in K) on the epitaxial strain, according to Eq. (5).

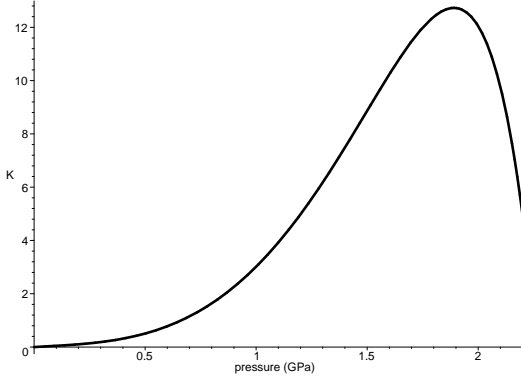


Fig. 4. Theoretical variation of the critical temperature $T_c - T_c^0$ (in K) on applied hydrostatic pressure, according to Eq. (5).

pressure. This function is plotted in Fig. 4, which displays the characteristic maximum of T_c versus pressure, as observed experimentally [1]. Note that the numerical agreement with experimental data in this case is poorer than for epitaxial strain.

Remark 5 For small strains, an approximate phenomenological expression for T_c as a function of the applied strain, widely used in the literature, is

$$T_c = T_c^0 + A(\varepsilon_{aa} + \varepsilon_{bb}) + B\varepsilon_{cc}, \quad (8)$$

where, for LSCO, $A = -284$ K and $B = 851$ K (notably, $A < 0$, $B > 0$). The latter expression may be viewed as a linear approximation to (5), with $A = \left. \frac{\partial T_c}{\partial \varepsilon_{aa}} \right|_0 = \left. \frac{\partial T_c}{\partial \varepsilon_{bb}} \right|_0$, and $B = \left. \frac{\partial T_c}{\partial \varepsilon_{cc}} \right|_0$.

Therefore, the critical temperature is a *decreasing* function of the horizontal macroscopic strain, which seems to be in contradiction with the fact that, in Eq. (4), T_c is an *increasing* function of the horizontal microstrains p_a and p_b (recall in fact that $p_a = \varepsilon_{aa}$, $p_b = \varepsilon_{bb}$). This may be explained by noting that the apical microstrain p_{api} is a very

fast decreasing function of the horizontal strain ($\varepsilon_{aa}, \varepsilon_{bb}$) [12], and it prevails quantitatively in Eq. (4) over the horizontal microstrains. Thus, according to Eq. (4), the observed decrease of the critical temperature under uniaxial horizontal strain (as measured by the negative A) seems to be essentially due to the accompanying decrease of the apical distance.

3 Microscopic model

We start by considering the following Hubbard-like Hamiltonian for an interacting electron system on a 2D square lattice [28]

$$H = \sum_{\mathbf{k}\sigma} \xi_{\mathbf{k}} c_{\mathbf{k}\sigma}^\dagger c_{\mathbf{k}\sigma} + \frac{1}{N} \sum_{\mathbf{k}\mathbf{k}'} V_{\mathbf{k}\mathbf{k}'} c_{\mathbf{k}\uparrow}^\dagger c_{-\mathbf{k}\downarrow}^\dagger c_{-\mathbf{k}'\downarrow} c_{\mathbf{k}'\uparrow}. \quad (9)$$

Here, $c_{\mathbf{k}\sigma}^\dagger$ ($c_{\mathbf{k}\sigma}$) is a creation (annihilation) operator for an electron state with wavevector \mathbf{k} and spin projection $\sigma \in \{\uparrow, \downarrow\}$, N is the number of lattice sites, and the sums are restricted to the first Brillouin zone (1BZ). We assume the electron-electron interaction in the separable form $V_{\mathbf{k}\mathbf{k}'} = \lambda g_{\mathbf{k}} g_{\mathbf{k}'}$, where $g_{\mathbf{k}} = \frac{1}{2}(\cos k_x - \cos k_y)$ is the lowest-order d -wave lattice harmonic for a square lattice, and λ a phenomenological coupling constant ($\lambda < 0$).

Detailed band structure calculations [29] as well as ARPES [30] suggest that a tight-binding approximation for the dispersion relation $\xi_{\mathbf{k}}$ of most high- T_c cuprates should retain at least nearest (NN, t) and next-nearest neighbors (NNN, t') hopping. We then assume the following rigid band-dispersion relation for LSCO:

$$\xi_{\mathbf{k}} = -2t(\cos k_x + \cos k_y) + 4t' \cos k_x \cos k_y - \mu, \quad (10)$$

where μ denotes the chemical potential, and the components of the wavevector \mathbf{k} are measured in units of the inverse lattice spacing. In order to have a flat minimum in $\xi_{\mathbf{k}}$ around the Γ point, as observed experimentally [30], the condition $0 < r < \frac{1}{2}$ must be fulfilled. A nonzero value of the hopping ratio $r = t'/t$ destroys perfect nesting at $\mu = 0$ as well as the electron-hole symmetry, and is known to stabilize superconductivity against other possible low-energy instabilities [31].

As the chemical potential μ in Eq. (10) varies from the bottom, $\varepsilon_{\perp} = -4t(1 - r)$, to the top of the band, $\varepsilon_{\top} = 4t(1 + r)$, the Fermi line $\xi_{\mathbf{k}} = 0$ evolves from an electron-like contour, closed around the Γ point, to a hole-like contour, whose continuation into higher Brillouin zones closes around the $M = (\pi, \pi)$ point (see also Fig. 7 below). In doing so, an ETT is traversed at $\mu = \varepsilon_c = -4t'$, where the Fermi line touches the zone boundaries.

It is worth emphasizing that the assumed d -wave momentum dependence of the potential energy correlates in a nontrivial way with the behaviour of the Fermi line close to the ETT. Indeed, the above choice for the pairing potential yields a gap energy $\Delta_{\mathbf{k}} \propto g_{\mathbf{k}}$, with maximum amplitudes occurring at $X = (0, \pi)$ (and symmetry related points), *i.e.* exactly at the ETT. Moreover, this is where the shape of the Fermi line is most sensible to changes in

the hopping ratio r [32]. Therefore, a deformation of the Fermi line induces a change of the phase space effectively probed by the electron-electron interaction [33]. This is particularly relevant in the case of anisotropic pairing with d -wave symmetry, such as that mediated by the exchange of antiferromagnetic spin density wave [34] or charge density wave fluctuations [35], as well as in the case of d -wave pairing enhanced by interlayer pair-tunneling [36,37].

An ETT gives rise to anomalous behaviors in the normal as well as in the superconducting properties of the electron system, as a function of the distance $z = \mu - \varepsilon_c$ from the ETT [13,14,15]. At variance with the 3D case, a 2D superconductor close to an ETT is characterized by a nonmonotonic dependence of T_c on z , as observed experimentally as a function of doping [38], or hydrostatic pressure [1]. Such a result has been recently rederived analytically [19,20]. Moreover, one finds that T_c at optimal doping (*i.e.*, near the ETT) correlates directly with the hopping ratio r , both for an s - and for a d -wave superconductor [19,20], as is extracted from band structure calculations for several hole-doped high- T_c cuprates [39].

The effects of the proximity to an ETT in the normal state are more difficult to be detected. For example, it is well known that the presence of an ETT at $T = 0$ gives rise to a peak in the thermoelectric power of a metal as well as to minima in the voltage-current characteristic of a tunnel junction [13]. However, the increase of temperature is expected to smear such effects. On the other hand, the sign change of the Hall resistivity R_H in the cuprates as a function of doping [40] (see also Ref. [41] for measurements of R_H in LSCO thin films) has been related to the presence of a Van Hove singularity in the single-particle spectrum of LSCO [42] (see also Ref. [15] for a review). Indeed, it has been shown that the sign of the Hall conductivity correlates with $\partial \ln T_c / \partial \ln \mu$ [43], which in particular implies a sign change at optimal doping, *i.e.* near the ETT.

In order to understand the nonmonotonic dependence of the critical temperature T_c as a function of lattice strain, we argue that a strain-induced deformation of the lattice varies the parameters in Eq. (10), so that T_c attains its optimal value close to the ETT. To this aim, one has to recognize that applied pressure (hydrostatic pressure or anisotropic stress) can in principle modify all the parameters in the model, so that several contributions to the overall pressure dependence of T_c can be identified [44]. In particular, pressure is expected to modify the overall hole doping level δ . Moreover, an intrinsic source of variation for T_c is expected to come from the dependence of the hopping parameters as well as of the coupling constant on the lattice spacings. In Ref. [44], a phenomenological dependence of the hopping parameters as well as the coupling constant on hydrostatic pressure has been assumed [44]. Here, we restrict to the case $\delta = \text{const}$, and argue that the main parameter driving the deformation of the Fermi line in the case of in-plane epitaxial strain be the hopping ratio r .

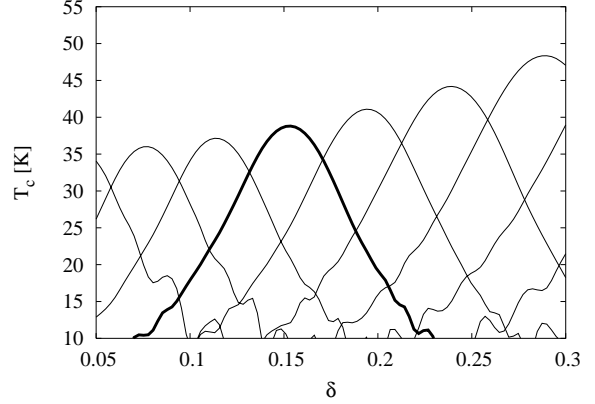


Fig. 5. Critical temperature T_c as a function of hole doping δ , Eq. (12), for fixed hopping ratio $r = t'/t = 0 \div 0.5$ ($t = 0.4$ eV, $\lambda = -0.45$ eV). Along each curve, one recovers the typical bell-shaped dependence of T_c on δ , the maximum occurring close to the ETT. The thicker line corresponds to $r = 0.182$, for which T_c attains a maximum of ≈ 40 K for $\delta \approx 0.15$, as observed experimentally for LSCO.

4 Numerical results and discussion

A standard mean-field approximation of Eq. (9) yields the BCS gap equation [28,44]:

$$\Delta_{\mathbf{k}} = -\frac{1}{N} \sum_{\mathbf{k}'} V_{\mathbf{k}\mathbf{k}'} \chi_{\mathbf{k}'} \Delta_{\mathbf{k}'}, \quad (11)$$

where $\Delta_{\mathbf{k}} \equiv \Delta g_{\mathbf{k}}$ is the gap energy, $\chi_{\mathbf{k}} = (2E_{\mathbf{k}})^{-1} \tanh(\frac{1}{2}\beta E_{\mathbf{k}})$ the pair susceptibility, $E_{\mathbf{k}} = \sqrt{\xi_{\mathbf{k}}^2 + \Delta_{\mathbf{k}}^2}$ the upper branch of the superconducting excitation spectrum, and $\beta = (k_B T)^{-1}$ the inverse temperature. Eq. (11) must be supplemented by the equation defining the band filling n , or equivalently the hole doping $\delta = 1 - n$,

$$n = 1 - 2 \sum_{\mathbf{k}} \xi_{\mathbf{k}} \chi_{\mathbf{k}}. \quad (12)$$

At $T = T_c$, $\Delta \rightarrow 0$, and Eq. (11) can be linearized as

$$1 + \lambda \frac{1}{N} \sum_{\mathbf{k}} g_{\mathbf{k}}^2 \chi_{\mathbf{k}}^c = 0, \quad (13)$$

where $\chi_{\mathbf{k}}^c = (2\xi_{\mathbf{k}})^{-1} \tanh(\beta_c \xi_{\mathbf{k}}/2)$. Eqs. (13) and (12) can be solved self-consistently for the critical temperature T_c and the chemical potential μ , at fixed hole content δ , for a given hopping ratio r .

Figs. 5 and 6 show our numerical results for T_c as a function of δ , for fixed values of the hopping ratio r in the meaningful range $0 \div 0.5$, and for T_c as a function of r , for fixed hole content δ , respectively ($t = 0.4$ eV, $\lambda = -0.45$ eV, yielding an optimal $T_c \approx 40$ K at $\delta \approx 0.15$ for $r \approx 0.2$, as observed experimentally in LSCO).

In Fig. 5, each curve corresponds to a given band dispersion relation, Eq. (10), fixed by a constant value of the hopping ratio r . The topology of the Fermi line $\xi_{\mathbf{k}} = 0$ evolves from a hole-like to an electron-like contour as δ

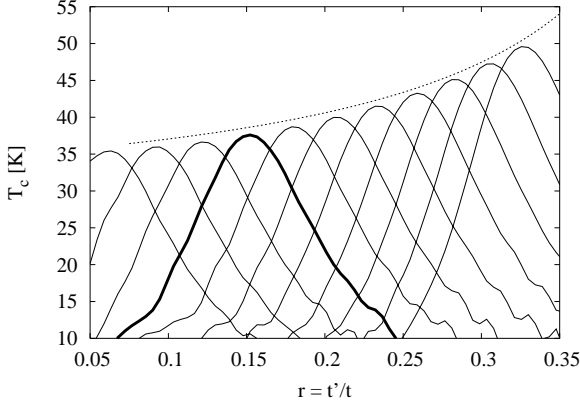


Fig. 6. Critical temperature T_c as a function of hopping ratio $r = t'/t$ (other parameters as in Fig. 5). Along each curve, $\delta = \text{const}$ ($\delta = 0.05 \div 0.3$, as in Fig. 5; the thicker line corresponds to $\delta = 0.125$). One recognizes a nonmonotonic dependence of T_c on strain, as observed experimentally, the maximum in T_c being attained close to the ETT. One also recovers the direct correlation between T_c^{max} on each curve and the hopping ratio r (dashed line, vertically shifted, for clarity) [39, 19, 20].

increases (μ decreases), as depicted in Fig. 7 (left). Here, the ETT is driven by a variation of the hole content δ , which in turn implies a change in chemical potential μ , through Eq. (12). For a given band structure ($r = \text{const}$), one recognizes the typical bell-shaped dependence of T_c on doping, as observed experimentally [38, 1]. A maximum in T_c is found close, though not exactly at, the ETT [19, 20].

On the other hand, epitaxial strain in thin films may realize the conditions assumed in Fig. 6, *viz.* a modification of the lattice spacings induce a variation of the hopping parameters in Eq. (10), and therefore in the hopping ratio r . Here, we assume that we can neglect the strain dependence of the NN hopping parameter t , mainly fixing the scale for T_c , compared to that of the NNN hopping parameter t' , whose value determines the actual shape of the Fermi line at the ETT. Indeed, within the extended Hückel theory [45], the hopping parameters t and t' can be roughly approximated by the overlap integrals between NN Cu $3d_{x^2-y^2}$ and O $2p_x$ orbitals, and NNN O $2p_x$ and O $2p_y$ orbitals, respectively (see Fig. 1 in Ref. [39]). Due to the weaker overlap of the latter two orbitals, it is to be expected that for moderate strain t' increases much faster than t as the CuO₂ unit cell is compressed, provided that the tetragonal symmetry of the lattice is preserved [44]. We can also neglect the strain dependence of the hole content δ , which in the case of LSCO close to optimal doping is known to be weakly dependent on hydrostatic pressure [46]. On the other hand, our main conclusions should not be affected by a strain-dependent coupling constant λ (see, however, Ref. [44]).

Fig. 6 displays our numerical results for T_c as a function of the hopping ratio $r = t'/t$. Each curve corresponds to a constant value of the hole doping δ . Assuming an approximately linear dependence of the hopping ratio r on the in-plane microscopic strain $\varepsilon_{aa} = \varepsilon_{bb}$, and neglecting

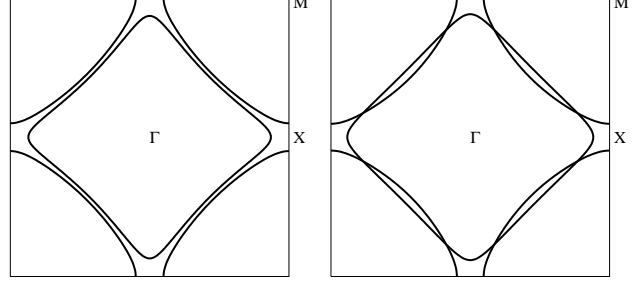


Fig. 7. Typical Fermi lines $\xi_{\mathbf{k}} = 0$, Eq. (10), at either side of an ETT. *Left:* The ETT is driven by a variation of the hole content δ , at constant r ($r = 0.182$, corresponding to the thicker plot in Fig. 5). *Right:* The ETT is driven by a (strain-induced) variation of the hopping ratio r , at constant δ ($\delta = 0.125$, thicker plot in Fig. 6). In both cases, the Fermi line changes topology, from a hole-like contour, centered around the $M = (\pi, \pi)$ point, to an electron-like contour, centered around the Γ point.

the strain dependence of all other parameters, one recovers a nonmonotonic dependence of T_c on strain, as observed experimentally, in agreement with the phenomenological model of Sec. 2. In particular, the maximum in T_c is attained close to the ETT. At variance with the case considered in Fig. 5, the topology change of the Fermi line at fixed hole doping is here driven by a strain-induced variation of the band parameters (Fig. 7, right). One also recovers the direct correlation between the critical temperature at optimal doping for each curve, T_c^{max} , and the hopping ratio r (Fig. 6, dashed line), as analytically found in Ref. [19, 20], and observed experimentally for many high- T_c cuprates [39].

5 Conclusions

Within a Ginzburg-Landau approach, we have proposed a phenomenological model for the critical temperature T_c as a function of microscopic strain ε in a tetragonal cuprate superconductor. For small strains, the model predicts an increase of T_c when the size of the CuO octahedron increases. Such a behavior is rather generic to high- T_c superconductors, as has been very recently confirmed by the observed increase of T_c up to 117 K in lattice-expanded doped fullerites [3].

On the other hand, for fixed in-plane or apical strains, T_c displays a nonmonotonic behavior on either apical or in-plane microstrains, respectively. Such a behavior is recovered also for the dependence of T_c on hydrostatic pressure P , in agreement with the T_c vs. P plots of most cuprate compounds [1]. Moreover, under epitaxial strain, we find a monotonically decreasing T_c in the experimentally accessible range $-0.006 \leq \varepsilon_{\text{epi}} \leq 0.006$, with a sharp maximum just below the lower bound of the mentioned range, in good qualitative and quantitative agreement with the experimental results for epitaxially strained LSCO [5, 26].

From a microscopic point of view, a nonmonotonic strain dependence of the critical temperature in the high- T_c cuprates has been interpreted as due to the proximity to an electronic topological transition (ETT). The quasi-2D band structure generic to cuprates implies a topology change of the Fermi line $\xi_{\mathbf{k}} = 0$, evolving from a hole-like to an electron-like contour in the 1BZ. A variation (in the most general sense of variational calculus) of the band-dispersion $\xi_{\mathbf{k}}$ induces a change in various observable properties, such as T_c (thus, a *functional* of $\xi_{\mathbf{k}}$), with a maximum occurring at, or close to, the ETT.

Assuming a tight-binding parametrization of the band structure, one way to ‘vary’ $\xi_{\mathbf{k}}$ is that of changing the hole content. Physically, this is what is most commonly realized by doping in the experiments, and what has been usually considered in the theoretical literature [16,17]. Such a situation corresponds to the assumption of a *rigid* band, namely an electronic band whose structure does not depend on its filling.

Here, we considered another class of ‘variations’ of $\xi_{\mathbf{k}}$, *i.e.* a change in the band parameters, at fixed hole content. A modification of the in-plane band parameters can be induced by in-plane epitaxial strain, through a change in the lattice spacings, without perturbing the tetragonal symmetry of the lattice. The idea of an ETT driven by a modification of the band structure, at fixed hole content, as contrasted to an ETT induced by doping or hydrostatic pressure for a rigid band, is particularly relevant for LSCO, where the hole content is known to be practically independent of pressure [46].

Thus, a numerical analysis of a minimal microscopic model for d -wave superconductivity close to an ETT allowed us to recover a nonmonotonic dependence of T_c on the hopping ratio r , measuring the distortion of the electronic band under in-plane epitaxial strain. At constant doping, a variation of r modifies the topology of the Fermi line and drives an electronic topological transition, with T_c attaining the maximum value close to the ETT. Such a result enables us to justify, from a microscopic point of view, the proposed phenomenological model for T_c as a function of microstrain in the cuprates.

G.G.N.A. acknowledges partial support from the E.U. through the F.S.E. Program. P.C. and P.P.G. acknowledge partial support from the M.U.R.S.T. through Progetto Cofinanziato 2000 “Modelli Matematici per la Scienza dei Materiali”; from the E.U. through the TMR Contract FMRX-CT98-0229 “Phase Transitions in Crystalline Solids”; and from the GNFM (INDAM), Contract “Effetti della deformazione sulla temperatura critica dei superconduttori.”

References

1. R. J. Wijngaarden, D. Tristan Jover, and R. Griessen, *Physica B* **265**, 128 (1999).
2. L. Gao, Y. Y. Xue, F. Chen, Q. Xiong, R. L. Meng, D. Ramirez, C. W. Chu, J. Eggert, and H. K. Mao, *Physica C* **235-240**, 1493 (1994).
3. J. H. Schön, Ch. Kloc, and B. Batlogg, *Science* **293**, 2432 (2001).
4. I. E. Trofimov, L. A. Johnson, K. V. Ramanujachary, S. Guha, M. G. Harrison, M. Greenblatt, M. Z. Cieplak, and P. Lindenfild, *Appl. Phys. Lett.* **65**, 2481 (1994).
5. J.-P. Locquet, J. Perret, J. Fompeyrine, E. Machler, J. W. Seo, and G. Van Tendeloo, *Nature* **394**, 453 (1998).
6. H. Sato and M. Naito, *Physica C* **274**, 221 (1997).
7. Weidong Si and X. X. Xi, *Appl. Phys. Lett.* **78**, 240 (2001).
8. H. Sato, A. Tsukada, M. Naito, and A. Matsuda, *Phys. Rev. B* **61**, 12447 (2000).
9. X. J. Chen, H. Q. Lin, and C. D. Gong, *Phys. Rev. B* **61**, 9782 (2000).
10. A. Bianconi, G. Bianconi, S. Caprara, D. Di Castro, H. Oyanagi, and N. L. Saini, *J. Phys.: Condens. Matter* **12**, 10655 (2000).
11. Weidong Si, Hong-Cheng Li, and X. X. Xi, *Appl. Phys. Lett.* **74**, 2839 (1999).
12. P. Cermelli and P. Podio-Guidugli, *Physica C* ..., ... (2001).
13. A. A. Varlamov, V. S. Egorov, and A. V. Pantsulaya, *Adv. Phys.* **38**, 469 (1989).
14. Ya. M. Blanter, M. I. Kaganov, A. V. Pantsulaya, and A. A. Varlamov, *Phys. Rep.* **245**, 159 (1994).
15. R. S. Markiewicz, *J. Phys. Chem. Solids* **58**, 1179 (1997).
16. F. Onufrieva, P. Pfeuty, and M. Kiselev, *Phys. Rev. Lett.* **82**, 2370 (1999).
17. F. Onufrieva and P. Pfeuty, *Phys. Rev. Lett.* **82**, 3136 (1999), [*Phys. Rev. Lett.* **83**, 1271 (1999)].
18. A. Ino, C. Kim, M. Nakamura, T. Yoshida, T. Mizokawa, Z.-W. Shen, A. Fujimori, T. Kakeshita, H. Eisaki, and S. Uchida, *Phys. Rev. B* ..., ... (2001), preprint `cond-mat/0005370`.
19. G. G. N. Angilella, E. Piegari, and A. A. Varlamov, submitted to *Phys. Rev. B* (unpublished).
20. G. G. N. Angilella, E. Piegari, R. Pucci, and A. A. Varlamov, in *Frontiers of high pressure research II: Application of high pressure to low-dimensional novel electronic materials*, Vol. 48 of *NATO Science Series*, edited by H. D. Hochheimer, B. Kuchta, P. K. Dorhout, and J. L. Yarger (Kluwer, Dordrecht, 2001).
21. U. Welp, M. Grimsditch, S. Fleshler, W. Nessler, J. Downey, G. W. Crabtree, and J. Guimpel, *Phys. Rev. Lett.* **69**, 2130 (1992).
22. S. L. Bud'ko, J. Guimpel, O. Nakamura, M. B. Maple, and I. K. Schuller, *Phys. Rev. B* **46**, 1257 (1992).
23. W. E. Pickett, *Phys. Rev. Lett.* **78**, 1960 (1997).
24. V. G. Tissen, Yonga Wang, A. P. Paulikas, B. W. Veal, and J. S. Schilling, *Physica C* **316**, 21 (1999).
25. N. Yamada and E. M. Ido, *Physica C* **203**, 240 (1992).
26. J.-P. Locquet, J. Perret, J. W. Seo, and J. Fompeyrine, in *Superconducting and related oxides: physics and nano-engineering III*, Vol. 3481 of *Proceedings of SPIE*, edited by D. Pavuna and I. Bozovic (SPIE, Bellingham, Washington, 1998), p. 248.
27. X. F. Chen, G. X. Tessema, and M. J. Skove, *Physica C* **181**, 340 (1991).
28. R. Fehrenbacher and M. R. Norman, *Phys. Rev. Lett.* **74**, 3884 (1995).
29. O. K. Andersen, A. I. Liechtenstein, O. Jepsen, and F. Paulsen, *J. Phys. Chem. Solids* **56**, 1573 (1995).
30. Z.-X. Shen and D. S. Dessau, *Phys. Rep.* **253**, 1 (1995).
31. J. V. Alvarez and J. González, *Europhys. Lett.* **44**, 641 (1998).

- 32. R. Hlubina and T. M. Rice, *Phys. Rev. B* **51**, 9253 (1995).
- 33. C. Hodges, H. Smith, and J. W. Wilkins, *Phys. Rev. B* **4**, 302 (1971).
- 34. A. J. Millis, H. Monien, and D. Pines, *Phys. Rev. B* **42**, 167 (1990).
- 35. A. Perali, C. Castellani, C. Di Castro, and M. Grilli, *Phys. Rev. B* **54**, 16216 (1996).
- 36. S. Chakravarty, A. Sudbø, P. W. Anderson, and S. Strong, *Science* **261**, 337 (1993).
- 37. G. G. N. Angilella, R. Pucci, F. Siringo, and A. Sudbø, *Phys. Rev. B* **59**, 1339 (1999).
- 38. H. Zhang and H. Sato, *Phys. Rev. Lett.* **70**, 1697 (1993).
- 39. E. Pavarini, I. Dasgupta, T. Saha-Dasgupta, O. Jepsen, and O. K. Andersen, *Phys. Rev. Lett.* **87**, 047003 (2001).
- 40. K. Tamasaku, T. Ito, H. Takagi, and S. Uchida, *Phys. Rev. Lett.* **72**, 3088 (1994).
- 41. J.-P. Locquet, Y. Jaccard, A. Cretton, E. J. Williams, F. Arrouy, E. Mächler, T. Schneider, Ø. Fischer, and P. Martinoli, *Phys. Rev. B* **54**, 7481 (1996).
- 42. A. Avella, F. Mancini, and D. Villani, *Sol. State Commun.* **108**, 723 (1998).
- 43. A. G. Aronov, S. Hikami, and A. I. Larkin, *Phys. Rev. B* **51**, 3880 (1995).
- 44. G. G. N. Angilella, R. Pucci, and F. Siringo, *Phys. Rev. B* **54**, 15471 (1996).
- 45. R. Hoffmann, *J. Chem. Phys.* **39**, 1397 (1963).
- 46. C. Murayama, Y. Iye, T. Enomoto, N. Mori, Y. Yamada, T. Matsumoto, Y. Kubo, Y. Shimakawa, and T. Manako, *Physica C* **183**, 277 (1991).